

Predicting EGFR Mutation Status by a Deep Learning Approach in Patients with Non-Small Cell Lung Cancer Brain Metastases

Oz Haim

Tel Aviv Ichilov-Sourasky Medical Center: Tel Aviv Sourasky Medical Center <https://orcid.org/0000-0003-0872-6263>

Shani Abramov

Tel Aviv Ichilov-Sourasky Medical Center: Tel Aviv Sourasky Medical Center

Ben Shofty

baylor college of medicine department of neurosurgery

Claudia Fanizzi

Fondazione IRCCS Istituto Neurologico Carlo Besta

Francesco DiMeco

Fondazione IRCCS Istituto Neurologico Carlo Besta

Netanell Avisdris

Tel Aviv University Sagol School of Neuroscience

Zvi Ram

Tel Aviv Ichilov-Sourasky Medical Center: Tel Aviv Sourasky Medical Center

Moran Artzi

Tel Aviv University Sagol School of Neuroscience

Rachel Grossman (✉ rachelyg@hotmail.com)



Tel Aviv Ichilov-Sourasky Medical Center: Tel Aviv Sourasky Medical Center

Research Article

Keywords: NSCLC, brain, metastasis, EGFR, MRI, deep learning

Posted Date: November 8th, 2021

DOI: <https://doi.org/10.21203/rs.3.rs-1020480/v1>

License:   This work is licensed under a Creative Commons Attribution 4.0 International License. [Read Full License](#)

Version of Record: A version of this preprint was published at Journal of Neuro-Oncology on February 4th, 2022. See the published version at <https://doi.org/10.1007/s11060-022-03946-4>.

Abstract

PURPOSE: Non-small cell lung cancer (NSCLC), the most prevalent subtype of lung cancer, tends to metastasize to the brain. Between 10-60% of NSCLCs harbor an activating mutation in the epidermal growth factor receptor (EGFR), which may be targeted with selective EGFR inhibitors. However, due to a high discordance rate between the molecular profile of the primary tumor and the brain metastases (BMs), identifying an individual patient's EGFR status of the BMs necessitates tissue diagnosis via an invasive surgical procedure. We employed a deep learning (DL) method with the aim of noninvasive detection of the EGFR mutation status in NSCLC BM.

METHODS: We retrospectively collected clinical, radiological, and pathological-molecular data of all the NSCLC patients who had been diagnosed with BMs and underwent resection of their BM during 2006-2019. The study population was then divided into 2 groups based upon EGFR mutational status. We further employed a DL technique to classify the 2 groups according to their preoperative magnetic resonance imaging features. Finally, we established the accuracy of our model in predicting EGFR mutation status of BM of NSCLC.

RESULTS: Fifty-nine patients were included in the study, 16 patients harbored EGFR mutations. Our model predicted mutational status with mean accuracy of 89.8%, sensitivity of 68.7%, specificity of 97.7%, and a receiver operating characteristic curve)ROC(value of 0.91 across the 5 validation datasets.

CONCLUSION: DL based noninvasive molecular characterization is feasible, has high accuracy and should be further validated in large prospective cohorts.

Introduction

Lung cancer is the most commonly diagnosed type of cancer and the leading cause for cancer-associated mortality worldwide, with an incidence of 2.1 million new cases each year [1]. Non-small cell lung cancer (NSCLC) is the most prevalent among the lung cancer subtypes, accounting for about 85% of cases [2]. Brain metastases (BMs) are the most common intracranial neoplasm, and lung cancer is their main source [3]. Between 10-50% of NSCLC metastasize to the brain, depending upon characteristics of the primary tumor such as stage, molecular profile, and previous oncological treatments [4, 5]. Historically, patients with BMs were considered to have a very poor prognosis, with a median survival rate of 1-3 months [6]. Recent progress in this field has led to much improvement in survival in selected cases amenable to the new generation therapies [6].

Many genetic alterations have been found in NSCLC tumors, and the most fundamental driver mutations among them is the activation of mutations of the epidermal growth factor receptor (EGFR). EGFRs are proteins located on the cell membrane, and their endpoint is cell proliferation, which is activated in part by a cascade of tyrosine kinase signaling [7]. Activating mutations of EGFR are observed between 10-60% of NSCLC patients, influenced, among other factors, by geographic and ethnic characteristics [8]. Targeted therapy against EGFR, a subset of tyrosine kinase inhibitors (TKI) has recently replaced standard chemotherapy as first-line treatment in advanced metastatic NSCLC with improved response rates [9–11],

even among the subgroup of patients with BMs [12]. Unfortunately, resistance to EGFR TKIs is not uncommon, as manifested in some cases by restoration of a wild-type EGFR profile [13]. Moreover, there is 30-55% of discordance between the molecular profile of the primary tumor and its BMs, thus making it impossible to extrapolate the EGFR status of the BMs from the original tumor source [14–16].

Although knowing the EGFR status of each BM is crucial for treatment planning, it had been possible only via the information derived from a tumor specimen. Tailoring specific treatments for different mutations of NSCLC and diagnose changes in their molecular profile by radiological tools, may preclude the need for invasive procedures.

In recent years there has been significant progress in the use of artificial intelligence methods in the form of conventional machine learning [17] and deep learning (DL) for medical image analysis [18]. Indeed DL methodologies have become the state-of-the-art approach in various computer imaging capabilities, with extensive applications in medical image analysis [19–21]. Several studies have investigated the feasibility of conventional machine learning methods for the differentiation of NSCLC molecular subtypes, 2 of which targeted BM and used a radiomics approach [22, 23]. While radiomics has been suggested to have a real clinical impact in lung cancer [24], it also harbors some structured limitations [25, 26].

To the best of our knowledge, there has not been any analysis in which DL tools were assigned to delineate EGFR status in of BM in NSCLC patients. We therefore designed this work to apply DL analysis for this purpose.

Methods

Study Design

This experimental, analytic, comparative study aimed at assessing the reliability of a noninvasive tool for classifying BMs from an NSCLC source according to their EGFR status. Data were collected retrospectively from the medical files of the study population. Pathological data based on histology were extracted from pathological reports following tissue biopsy, and EGFR status, as part of the clinical process, was determined by reverse transcription polymerase chain reaction.

Study Population

We retrospectively collected the records of all NSCLC patients with BMs who underwent resection of their BMs in 2 institutions, Tel-Aviv Medical Center, Tel-Aviv, Israel between 2006-2019 (46 patients), and Fondazione IRCCS Istituto Neurologico C. Besta, Milan, Italy (13 patients). The patients were divided into 2 groups based upon their EGFR status of being positive or negative for EGFR mutation.

Included were all diagnosed NSCLC patients with BMs who underwent resection of their BMs and for whom a histology-based pathological report, the molecular-based EGFR status, and a preoperative magnetic resonance imaging (MRI) study of sufficient quality were available. Our analysis was restricted to specific

metastases which had been resected and for which their EGFR status had been determined. Preoperative MRI scans with major artifacts or of low quality, and scans of patients who had undergone radiation treatment to their BMs prior to the MRI were excluded. The study was approved by the local institutional review boards (IRB) in both centers, Tel-Aviv Medical Center, and Fondazione IRCCS Istituto Neurologico C. Besta, (IRB approval numbers 0200-10, and 81/2021, respectively).

Image Analysis

Preprocessing

Analysis was performed on the post contrast T1 weighted MRI images (T1W+c), and included bias field correction with an intensity inhomogeneity correction algorithm (SPM, part of MATLAB R2019b) [27], and intensity normalization by the equation:
$$x_i = \frac{x_i - \mu}{\sigma}$$
 where x_i is the value of given voxel in the image, μ and σ are the mean and standard deviation of the brain extracted image. Tumor segmentation was performed by senior neurosurgeon and using commercial software (AnalyzeDirect 11.0) at the slice (2D) level. The extracted mask was then used to generate crop images (i.e., delimitation of the lesion mask and its surrounding).

Data splitting

The entire dataset was split at the subject level into 80% training and 20% validation datasets in a stratified 5-fold cross-validation manner proportional to group size, and ensuring that all images belonging to a given patient would be allocated to the same group.

DL analysis

DL model training and evaluation were performed by means of the Fast.ai framework built on top of the PyTorch environment [28].

The input data for the DL analysis were cropped images of the mid-tumor region and ± 2 slices (total of 5 slices), all extracted from the normalized T1W+c image and resized to a 96X96 image size (Fig. 1). Data augmentation was performed in order to increase the dataset size and variance, and it included random rotations, zooming, and contrast modification. In addition, mixup augmentation [29] was applied for combining training samples by means of their linear combinations.

A ResNet-50 [30] convolutional neural network was set as the network's architecture. Network training was carried out by means of F1 loss function with an initial learning rate of $4e^{-2}$ and a batch size of 32. The metric for evaluating the model during training was the F1 score. Data oversampling was employed in order to cope with the imbalanced datasets, enabling sampling of the 2 groups in roughly equal amounts.

Due to the relatively small data size that was available for this study a transfer learning was performed, the network was trained using a pre-trained ResNet-50 model, trained on an ImageNet data set as previously described in detail elsewhere [31, 32]. Training was performed with a total of 40 epochs while preserving the model which achieved the best level of accuracy during the process.

Post-processing of the predicted results was performed at the subject level by calculation of a predication score for the adjacent slices and tested based upon median, maximum, minimum, and mean metrics (Fig. 1).

The classification results were evaluated on the validation datasets, for each one of the 5-folds, using accuracy, precision, recall, F1 score and receiver- operating characteristic curve (ROC).

Results

Patient characteristics

Preoperative post-contrast T1-weighted images (T1WI+c) of 59 patients with NSCLC BMs were reviewed. Forty-three of those patients (62 ± 12 years old, 15 females) had a negative EGFR mutational status and 16 patients (62 ± 11 years old, 11 females) had a positive EGFR mutational status. The study patients' characteristics are summarized in Table 1. There were no significant differences between the positive and negative status groups except for female dominance in the EGFR mutant group and male dominance in EGFR wild-type group, $t = 2.403$, $p = 0.02$).

Classification Results

The 5-fold cross validation results are presented in Table 2. The best classification results were obtained by using the median metric for the post-processing of the predicted results, with an overall accuracy of 89.8%, a sensitivity of 68.7%, and a specificity of 97.7% for the detection of a positive EGFR mutation status. The mean and median metrics achieved similar results of a mean ROC of 0.91, while the variability was lower for the median metric (0.07) compared to the mean metric (0.09), indicating the stability of the median metric. While the specificity of all post-processing methods was same (97.7%), both best performing methods (median and mean) achieved better sensitivity (68.7%), indicating that some slices were more informative than others in the EGFR mutation status prediction task. Figure 2 shows an ROC curve for the classification for the best performing post-processing metric (median) between the positive and negative EGFR mutations. The mean ROC value across the 5 validation datasets was 0.91 ± 0.07 (Fig. 2).

Discussion

This study provides a proof of concept that DL analysis can be applied for the prediction of EGFR mutation status in NSCLC BMs. By extracting data from a limited number of patients ($n=59$), applying the above-described augmentation technics and the transfer learning approach, together with post-processing of the predicted results, we were able to classify the patients according to their EGFR mutation status. This allowed us to reach an overall accuracy of 89.8%, a sensitivity of 68.7%, and a specificity of 97.7% for the detection of a positive EGFR mutation status.

Looking forward, one should expect machine learning technologies to become an inseparable part of our diagnostic workup and decision-making process. Chest computerized tomographic (CT)-based radiomics

analysis was established as a ground-breaking tool for discriminating between different molecular subtypes of NSCLC (including EGFR, ALK and KRAS mutations) [33]. Oikonomou et al. used positron emission tomography-CT-based radiomics to predict response to stereotactic body radiotherapy in lung cancer patients. Those authors found radiomics as being the only predictor for local control [34]. Hosny et al. investigated the predictive value of DL for mortality risk stratification in NSCLC. They incorporated several datasets to build a database of 1200 patients, and applied convolutional neural networks based upon an analysis of CT scans to predict the response to radiation therapy and surgery. They reported area under the curve (AUC) values of 0.70 and 0.71, respectively, and succeeded in stratifying patients into low and high mortality risk following both radiotherapy ($p < 0.001$) and surgery ($p = 0.03$) using the same tool [35]. Trebeschi et al. showed that standard-of-care imaging may serve as a base for machine learning to predict response to immunotherapy in NSCLC and melanoma patients. Their radiomics-based prediction tool for anti PD-L1 response achieved an AUC up to 0.83 for patients with NSCLC, with a survival advantage of 25% at 1 year following treatment [36].

It is highly significant to have the ability to combine a comprehensive molecular profile of each involved site while minimizing the invasiveness of the diagnostic workup and providing tailored treatment in the setting of BMs. Ramón et al. used MRI-based radiomics tools to differentiate lung origin of BMs from breast and melanoma origins with an accuracy of 90% [37].

Two trials were recently conducted in the field of machine learning for the prediction of EGFR status in NSCLC BM. Ahn et al. applied MRI based radiomics on 210 metastases (61 patients, of whom 29 were EGFR positive according to their lung pathology findings) and reached a diagnostic accuracy of 86.7% (AUC 0.868) [22]. Park et al. reached a diagnostic accuracy and an AUC of 78.6% and 0.73, respectively, utilizing radiomics tools based upon MRI features of 99 BMs (51 patients, of whom 42 were EGFR positive as confirmed by biopsy of at least one of the BMs) [23]. While trying to demonstrate a proof of concept for radiomics prediction of EGFR status in NSCLC BMs, both of these trials assumed an identical molecular profile between the sampled tissue and the rest of the metastases, an assumption that has since been shown to be not necessarily accurate [13–15]. Moreover, radiomics analysis is based upon a handcrafted image processing pipeline which includes feature extraction, feature selection, and machine learning model building. Any small change in any one of these steps may impair its prediction accuracy and stability.

Our results demonstrated a promising potential of utilizing a DL approach based on standard clinical MRI for noninvasive assessment of EGFR mutation status in BM of NSCLC patients. Although less accurate than histology-based results, it might be useful for treating patients who are not suitable for surgery and for those with eloquent-seated lesions or poly-metastatic disease.

Study Limitations

The main limitation of this study derives from the relatively small number of patients. Our sample size stems partly from the stringent study inclusion criteria and the current trend to radiate upfront many of those patients without pathological diagnosis. This limitation apparently represents a real-world challenge

when attempting to conclusively verify the utility of DL for predicting EGFR mutation status in patients with BM from lung cancer.

Conclusions

Determining the molecular profile of NSCLC BMs non-invasively is feasible with standard imaging studies by applying a DL tool. This technology has the potential to improve the personalized treatment paradigm of these patients. Despite being trained on a small cohort of patients, our classifier accurately predicted EGFR mutations when compare to previous works. Further research based on larger cohorts from different centers in diverse communities is warranted in order to create a reliable tool for widespread clinical use.

Declarations

Funding. This research did not receive any specific grant from funding agencies in the public, commercial, or not-for-profit sectors.

Conflicts of interest/Competing interests. The authors declare no competing interests.

Availability of data and material. All the data in this study is available in Sagol Brain Institute, Tel Aviv Medical Center, Tel-Aviv, Israel.

Code availability. Not applicable.

Ethics approval. Tel-Aviv Medical Center, and Fondazione IRCCS Istituto Neurologico C. Besta, (IRB approval numbers 0200-10, and 81/2021, respectively).

Consent to participate. Not applicable.

Consent for publication. Not applicable.

Author Contributions: Oz Haim, Ben Shofty, Zvi Ram, Moran Arzi and Rachel Grossman contributed to the study conception and design. Material preparation and data collection were performed by Shani Abramov, Oz Haim and Claudia Fanzinni, analysis was performed by Moran Arzi and Netanel Avisridis. The first draft of the manuscript was written by Oz Haim and all authors commented on previous versions of the manuscript. All authors read and approved the final manuscript.

References

1. Bray F, Ferlay J, Soerjomataram I, et al (2018) Global cancer statistics 2018: GLOBOCAN estimates of incidence and mortality worldwide for 36 cancers in 185 countries. *CA Cancer J Clin* 68:394–424. <https://doi.org/10.3322/caac.21492>
2. Molina JR, Yang P, Cassivi SD, et al (2008) Non-small cell lung cancer: epidemiology, risk factors, treatment, and survivorship. *Mayo Clin Proc* 83:584–594. <https://doi.org/10.4065/83.5.584>

3. Schouten LJ, Rutten J, Huveneers HAM, Twijnstra A (2002) Incidence of brain metastases in a cohort of patients with carcinoma of the breast, colon, kidney, and lung and melanoma. *Cancer* 94:2698–2705. <https://doi.org/10.1002/cncr.10541>
4. Chi A, Komaki R (2010) Treatment of Brain Metastasis from Lung Cancer. *Cancers* 2:2100–2137. <https://doi.org/10.3390/cancers2042100>
5. Shin D-Y, Na II, Kim CH, et al (2014) EGFR Mutation and Brain Metastasis in Pulmonary Adenocarcinomas. *J Thorac Oncol* 9:195–199. <https://doi.org/10.1097/JTO.000000000000069>
6. Ali A, Goffin JR, Arnold A, Ellis PM (2013) Survival of patients with non-small-cell lung cancer after a diagnosis of brain metastases. *Curr Oncol Tor Ont* 20:e300-306. <https://doi.org/10.3747/co.20.1481>
7. Oda K, Matsuoka Y, Funahashi A, Kitano H (2005) A comprehensive pathway map of epidermal growth factor receptor signaling. *Mol Syst Biol* 1:E1–E17. <https://doi.org/10.1038/msb4100014>
8. Midha A, Dearden S, McCormack R (2015) EGFR mutation incidence in non-small-cell lung cancer of adenocarcinoma histology: a systematic review and global map by ethnicity (mutMapII). *Am J Cancer Res* 5:2892–2911
9. Mok TS, Wu Y-L, Thongprasert S, et al (2009) Gefitinib or Carboplatin–Paclitaxel in Pulmonary Adenocarcinoma. *N Engl J Med* 361:947–957. <https://doi.org/10.1056/NEJMoa0810699>
10. Rosell R, Carcereny E, Gervais R, et al (2012) Erlotinib versus standard chemotherapy as first-line treatment for European patients with advanced EGFR mutation-positive non-small-cell lung cancer (EURTAC): a multicentre, open-label, randomised phase 3 trial. *Lancet Oncol* 13:239–246. [https://doi.org/10.1016/S1470-2045\(11\)70393-X](https://doi.org/10.1016/S1470-2045(11)70393-X)
11. Sequist LV, Yang JC-H, Yamamoto N, et al (2013) Phase III Study of Afatinib or Cisplatin Plus Pemetrexed in Patients With Metastatic Lung Adenocarcinoma With *EGFR* Mutations. *J Clin Oncol* 31:3327–3334. <https://doi.org/10.1200/JCO.2012.44.2806>
12. Soria J-C, Ohe Y, Vansteenkiste J, et al (2018) Osimertinib in Untreated EGFR-Mutated Advanced Non-Small-Cell Lung Cancer. *N Engl J Med* 378:113–125. <https://doi.org/10.1056/NEJMoa1713137>
13. Kalikaki A, Koutsopoulos A, Trypaki M, et al (2008) Comparison of *EGFR* and *K-RAS* gene status between primary tumours and corresponding metastases in NSCLC. *Br J Cancer* 99:923. <https://doi.org/10.1038/sj.bjc.6604629>
14. Bozzetti C, Tiseo M, Lagrasta C, et al (2008) Comparison Between Epidermal Growth Factor Receptor (EGFR) Gene Expression in Primary Non-small Cell Lung Cancer (NSCLC) and in Fine-Needle Aspirates from Distant Metastatic Sites. *J Thorac Oncol* 3:18–22. <https://doi.org/10.1097/JTO.0b013e31815e8ba2>
15. Brastianos PK, Carter SL, Santagata S, et al (2015) Genomic characterization of brain metastases reveals branched evolution and potential therapeutic targets. *Cancer Discov* 5:1164–1177. <https://doi.org/10.1158/2159-8290.CD-15-0369>
16. Berger LA, Riesenberger H, Bokemeyer C, Atanackovic D (2013) CNS metastases in non-small-cell lung cancer: Current role of EGFR-TKI therapy and future perspectives. *Lung Cancer* 80:242–248. <https://doi.org/10.1016/j.lungcan.2013.02.004>

17. Shofty B, Artzi M, Shtrozberg S, et al (2020) Virtual biopsy using MRI radiomics for prediction of BRAF status in melanoma brain metastasis. *Sci Rep* 10:6623. <https://doi.org/10.1038/s41598-020-63821-y>
18. Quon JL, Bala W, Chen LC, et al (2020) Deep Learning for Pediatric Posterior Fossa Tumor Detection and Classification: A Multi-Institutional Study. *Am J Neuroradiol* 41:1718–1725. <https://doi.org/10.3174/ajnr.A6704>
19. Lundervold AS, Lundervold A (2019) An overview of deep learning in medical imaging focusing on MRI. *Z Für Med Phys* 29:102–127. <https://doi.org/10.1016/j.zemedi.2018.11.002>
20. Litjens G, Kooi T, Bejnordi BE, et al (2017) A survey on deep learning in medical image analysis. *Med Image Anal* 42:60–88. <https://doi.org/10.1016/j.media.2017.07.005>
21. Grossman R, Haim O, Abramov S, et al (2021) Differentiating Small-Cell Lung Cancer From Non-Small-Cell Lung Cancer Brain Metastases Based on MRI Using Efficientnet and Transfer Learning Approach. *Technol Cancer Res Treat* 20:15330338211004920. <https://doi.org/10.1177/15330338211004919>
22. Ahn SJ, Kwon H, Yang J-J, et al (2020) Contrast-enhanced T1-weighted image radiomics of brain metastases may predict EGFR mutation status in primary lung cancer. *Sci Rep* 10:. <https://doi.org/10.1038/s41598-020-65470-7>
23. Park YW, An C, Lee J, et al (2021) Diffusion tensor and postcontrast T1-weighted imaging radiomics to differentiate the epidermal growth factor receptor mutation status of brain metastases from non-small cell lung cancer. *Neuroradiology* 63:343–352. <https://doi.org/10.1007/s00234-020-02529-2>
24. Scrivener M, Jong EEC de, Timmeren JE van, et al (2016) Radiomics applied to lung cancer: a review. *Transl Cancer Res* 5:. <https://doi.org/10.21037/8536>
25. Li Q, Bai H, Chen Y, et al (2017) A Fully-Automatic Multiparametric Radiomics Model: Towards Reproducible and Prognostic Imaging Signature for Prediction of Overall Survival in Glioblastoma Multiforme. *Sci Rep* 7:14331. <https://doi.org/10.1038/s41598-017-14753-7>
26. Sun Q, Lin X, Zhao Y, et al (2020) Deep Learning vs. Radiomics for Predicting Axillary Lymph Node Metastasis of Breast Cancer Using Ultrasound Images: Don't Forget the Peritumoral Region. *Front Oncol* 10:. <https://doi.org/10.3389/fonc.2020.00053>
27. Ashburner J, Friston KJ (2005) Unified segmentation. *NeuroImage* 26:839–851. <https://doi.org/10.1016/j.neuroimage.2005.02.018>
28. Howard J, Gugger S (2020) Fastai: A Layered API for Deep Learning. *Information* 11:108. <https://doi.org/10.3390/info11020108>
29. Zhang H, Cisse M, Dauphin YN, Lopez-Paz D (2018) mixup: Beyond Empirical Risk Minimization. *ArXiv171009412 Cs Stat*
30. Liu W, Anguelov D, Erhan D, et al (2016) SSD: Single Shot MultiBox Detector. In: Leibe B, Matas J, Sebe N, Welling M (eds) *Computer Vision – ECCV 2016*. Springer International Publishing, Cham, pp 21–37
31. Iglovikov V, Shvets A (2018) TerausNet: U-Net with VGG11 Encoder Pre-Trained on ImageNet for Image Segmentation. *ArXiv180105746 Cs*
32. Lau SLH, Chong EKP, Yang X, Wang X (2020) Automated Pavement Crack Segmentation Using U-Net-based Convolutional Neural Network. *IEEE Access* 8:114892–114899.

<https://doi.org/10.1109/ACCESS.2020.3003638>

33. Chen B, Zhang R, Gan Y, et al (2017) Development and clinical application of radiomics in lung cancer. *Radiat Oncol* 12:154. <https://doi.org/10.1186/s13014-017-0885-x>
34. Oikonomou A, Khalvati F, Tyrrell PN, et al (2018) Radiomics analysis at PET/CT contributes to prognosis of recurrence and survival in lung cancer treated with stereotactic body radiotherapy. *Sci Rep* 8:4003. <https://doi.org/10.1038/s41598-018-22357-y>
35. Hosny A, Parmar C, Coroller TP, et al (2018) Deep learning for lung cancer prognostication: A retrospective multi-cohort radiomics study. *PLoS Med* 15:e1002711. <https://doi.org/10.1371/journal.pmed.1002711>
36. Trebeschi S, Drago SG, Birkbak NJ, et al (2019) Predicting response to cancer immunotherapy using noninvasive radiomic biomarkers. *Ann Oncol Off J Eur Soc Med Oncol* 30:998–1004. <https://doi.org/10.1093/annonc/mdz108>
37. Ortiz-Ramón R, Larroza A, Ruiz-España S, et al (2018) Classifying brain metastases by their primary site of origin using a radiomics approach based on texture analysis: a feasibility study. *Eur Radiol*. <https://doi.org/10.1007/s00330-018-5463-6>

Tables

Table 1: Clinical characteristics of NSCLC patients with BMs who underwent resection of their BMs.

Characteristics	EGFR wild type (N=43)		EGFR mutant (N=16)		P-value	
Age (years, Median \pm SD)	61.81 (11.82)		62.13 (10.65)		0.709	
Sex						
Male	28 (65%)		5 (31%)		0.02	
Female	15 (35%)		11 (69%)		0.02	
Location (involved lobe)	Lt.	Rt.	Lt.	Rt.	Lt.	Rt.
Frontal	20.4%	26.06%	24.75%	20.96%	0.680	0.658
Parietal	5.79%	1.35%	4.52%	9.77%	0.815	0.114
Temporal	6.79%	0.57%	1.11%	3.35%	0.230	0.188
Occipital	1.16%	2.09%	0.26%	0.12%	0.566	0.570
Limbic	5.55%	2.05%	0.48%	2.01%	0.076	0.983
Subcortical	6.58%	7.06%	6.43%	1.30%	0.977	0.244
Cerebellar	2.41%	11.75%	5.94%	19.01%	0.486	0.475
Brainstem	0.17%	0.22%	0%	0%	0.523	0.507
Tumor Volume (cm³, Mean \pm SD)						
T1WI+c	1.21 (0.58)		0.96 (0.52)		0.125	

Data are median (SD) or number (%).

Abbreviations: EGFR, epidermal growth factor receptor

Table 2: 5-Fold cross validation results for the different post-processing metrics.

Fold	Cross validation ROC					Overall ROC		At network result threshold 0.5		
	1	2	3	4	5	Mean	SD	Sensitivity	Specificity	Accuracy
Min	0.84	0.93	0.93	0.92	0.81	0.88	0.05	62.5%	97.7%	88.1%
Max	0.91	1.00	1.00	0.67	0.78	0.87	0.13	62.5%	97.7%	88.1%
Median	0.88	1.00	0.96	0.92	0.81	0.91	0.07	68.7%	97.7%	89.8%
Mean	0.94	1.00	1.00	0.83	0.78	0.91	0.09	68.7%	97.7%	89.8%

Abbreviations: ROC, receiver operating characteristic curve

Figures

Figure 1

Post-processing phase. The numbers for each slice indicating the predicted model EGFR score. Each post-processing metric was calculated based upon the 5-slice context scores.

Figure 2

Receiver operating characteristic, median slice metric, 5-fold combined. Abbreviations: ROC, receiver operating characteristic curve, ResNet, residual neural network.